ChemComm
Chemical Communications

Accepted Manuscript

This article can be cited before page numbers have been issued, to do this please use: W. Ai, Y. Gao, J. Xue, X. Liu, H. Liu, J. Wang and Y. Bai, *Chem. Commun.*, 2020, DOI: 10.1039/C9CC09629A.

ROYAL SOCIETY OF CHEMISTRY

rsc.li/chemcomm

View Article Online
DOI: 10.1039/C9CC09629A

COMMUNICATION

Tracing and Elucidating Visible-light Mediated Oxidation and C-H Functionalization of Amines Using Mass Spectrometry

Received 00th January 20xx,
Accepted 00th January 20xx

DOI: 10.1039/x0xx00000x

Wanpeng Ai,[a] Yunpeng Gao,[a] Jinjuan Xue,[a] Xiaoyun Liu,[b] Huwei Liu,[a] Jianbo Wang,[a] and Yu Bai*[a]

The co-existing mechanism of visible light mediated direct oxidation and C-H functionalization of amines was investigated by capturing all the intermediates using online mass spectrometry. The two-step dehydrogenation of amine involving in proton coupled electron transfer (PCET) process was revealed for the first time.

Cross-dehydrogenative coupling (CDC) reactions have emerged as a powerful tool for the efficient construction of C–C, C–N, C–O, and C–P bonds.[1-3] In particular, selective conversion of amines to amides through CDC is highly demanded in organic chemistry due to the ubiquity of amide bonds in various molecules, such as biological compounds and biopolymers.[4] Owing to the superiority of sustainability, green and mild condition, photoredox catalysis provides a promising replacement for the conventional organic synthesis[5-10]. Since Stephenson et al.[11] reported photocatalytic aza-Henry reaction of *N*-aryltetrahydroisoquinolines (THIQ) with nitromethane through CDC in 2010, visible light mediated direct oxidation and functionalization of C-H bond adjacent to nitrogen atom have been diversely explored[12-15].

In contrast to the rapid development of the photoredox oxidative transformations of amines, their mechanism investigations are lagged far behind. Efforts have been attempted using fluorescence quenching,[16] UV-vis absorption spectroscopy,[17, 18] transient absorption spectroscopy,[17-19] electron spin resonance (ESR)[16, 20] and NMR spectroscopy[21]. However, limited and indirect structural information of the transient intermediate, such as the radical cations, restrict the mechanism elucidation. Recently, electrospray ionization (ESI)[22-28,] desorption electrospray ionization (DESI)[29-35] and low-temperature plasma (LTP)[36] as well as electron impact (EI) coupling with temporal analysis of products (TAP) reactor[37-39] mass spectrometry (MS) have been applied in the reaction mechanism study, providing a highly sensitive tool for gaining detailed structural information of reactive intermediates through *in situ* detection. Through combination with the high power laser irradiance, the mechanism of dehydrogenation and [3 + 2] annulation have been elucidated[40 35]. The proposed mechanism of photoredox transformation of C-H bonds adjacent to nitrogen atom involves the formation of amine radical cation by single-electron-transfer (SET) and the subsequent H-abstraction by superoxide radical anion to form iminium cation. Thereafter, two pathways have been reported to convert iminium into different products, one is nucleophilic addition leading to functionalization of C-H bond adjacent to nitrogen, the other one is oxidation of iminium cation resulting in the formation of amide product. Even though co-existed pathways were proposed (Scheme S1)[12], no direct evidence for this mechanism of this significant photocatalytic reaction has been reported. To investigate the detailed mechanism of this process, ESI-MS assisted with laser irradiation setup was applied in our work to explore the visible-light mediated oxidation and C-H functionalization of THIQ (Scheme 1). Two new peroxide addition intermediates were detected and characterized, which disclosed the cascade stepwise aerobic oxidation to obtain amide products for the first time.

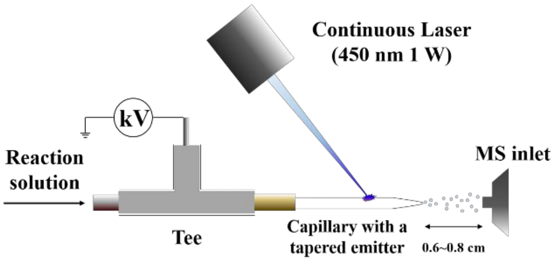

Scheme 1. Schematic illustration of the online ESI-MS assisted with laser irradiation setup.

---

[a] Beijing National Laboratory for Molecular Sciences, Key Laboratory of Bioorganic Chemistry and Molecular Engineering of Ministry of Education, College of Chemistry and Molecular Engineering, Peking University, Beijing 100871, P. R. China. E-mail: yu.bai@pku.edu.cn

[b] Department of Microbiology, School of Basic Medical Sciences, Peking University Health Science Center, Beijing 100191, China.

†Electronic Supplementary Information (ESI) available. See DOI: 10.1039/x0xx00000x

View Article Online
DOI: 10.1039/C9CC09629A

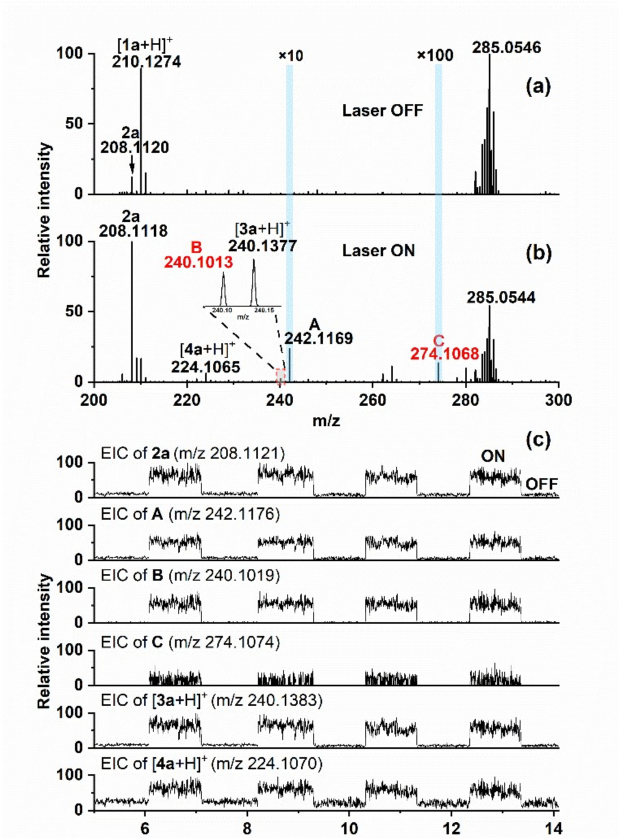

Figure 1. (a) MS spectrum of THIQ and [Ru(II)(bpy)$_3$]Cl$_2$ mixture, laser off; (b) MS spectrum of THIQ and [Ru(II)(bpy)$_3$]Cl$_2$ mixture, laser on; (c) Extracted ion chromatogram (EIC) of the related intermediates and products in (b).

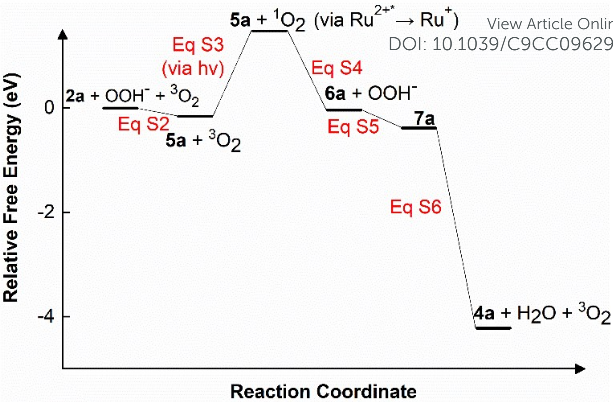

Figure 2. Relative free energy (considering solvation effect) profile of the two-step dehydrogenation pathway in Eq S2–S6 which are -0.156, 1.646, -1.524, -0.346, and -3.837 eV, respectively.

Table 1. MS peaks identification for THIQ and its related substances

	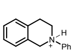 [**1a**+H]$^+$	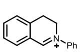 **2a**	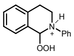 [**5a**+H]$^+$ (**A**)	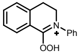 **6a** (**B**)
Chemical formula	$C_{15}H_{16}N^+$	$C_{15}H_{14}N^+$	$C_{15}H_{16}NO_2^+$	$C_{15}H_{14}NO_2^+$
Calculated *m/z*	210.1277	208.1121	242.1176	240.1019
Measured *m/z*	210.1274	208.1118	242.1169	240.1013
Error (ppm)	-1.4	-1.4	-2.9	-2.5
	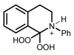 [**7a**+H]$^+$ (**C**)	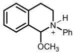 [**3a**+H]$^+$	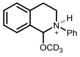 [**3a**-d_3+H]$^+$	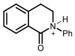 [**4a**+H]$^+$
Chemical formula	$C_{15}H_{16}NO_4^+$	$C_{16}H_{18}NO^+$	$C_{16}H_{15}D_3NO^+$	$C_{15}H_{14}NO^+$
Calculated *m/z*	274.1074	240.1383	243.1571	224.1070
Measured *m/z*	274.1068	240.1377	243.1566	224.1065
Error (ppm)	-2.2	-2.5	-2.1	-2.2

A mixture of THIQ **1a** (100 μM) and [Ru(II)(bpy)$_3$]Cl$_2$ (5 μM, bpy = 2,2'-bipyridine) in methanol was injected into the capillary with a tapered tip as the ESI spray needle with the flow rate of 10 μL/min. High power laser (450 nm, 1 W) was employed to irradiate the reaction mixture and trigger the photoredox catalysis reaction (Scheme 1 & Figure S3). For the clear demonstration of laser catalyzed reaction and the origin of the intermediates, the laser beam was turned on and off sequentially and repetitively at 1 min interval. When the laser was turned off, only ion of m/z 210.1274 and ion clusters with the dominant peak at m/z 285.0546 were detected, corresponding to the protonated **1a** and Ru^{2+}(bpy)$_3$, respectively (Figure 1a). It was noticed that a small peak of ions at m/z 208.1118 attributed to THIQ iminium cation (2-phenyl-3,4-dihydroisoquinolin-2-ium, **2a**) produced by in-source oxidation of **1a** during the ESI ionization process (Collision induced dissociation (CID) MS/MS spectrum, Figure S5). Once the laser was on, the signal of **2a** (m/z 208.1118) increased remarkably (Figure 1b), which certificated that **2a** came from the photocatalysis reaction. Ions at m/z 242.1169 (marked as **A**) was detected and further confirmed as the protonated 1-hydroperoxy-2-phenyl-1,2,3,4-tetrahydroisoquinoline **5a** by the formation of fragment ions at m/z 106 and 224 via losses of $C_8H_8O_2$ and H_2O in CID MS/MS spectrum (Figure S6). The above experimental results are consistent with those obtained by Bartling et al[21] using on-line NMR. Next, after setting the mass resolution to 280000, we were delighted to find that two peaks with very close m/z at 240.1377 and 240.1013 (marked as **B**) were successfully discriminated. According to the calculated molecule formula of $C_{16}H_{18}NO^+$ (error -2.5 ppm), m/z 240.1377 was proposed as the protonated ion of C-H methoxylated product 1-methoxy-2-phenyl-1,2,3,4-tetrahydroisoquinoline **3a**. To confirm this prediction, the deuterated methanol, methanol-d4, was employed to react with **1a** to avoid the close m/z and performed the CID MS/MS experiment. In its MS/MS spectrum, the dominant fragment ions at m/z 208 came from the loss of CD_3OH, which demonstrated that the ions at m/z 243.1566 arose from the deuterated **3a** (Figure S7). So far, our results detected and confirmed the pathway of nucleophilic addition based functionalization of C-H bond adjacent to nitrogen.

For the ambiguous oxidation pathway forming amide, more interestingly, two new peroxide addition intermediates were detected in our work (m/z 240.1013 (**B**) and 274.1068 (**C**), marked red in Figure 1b). The CID MS/MS was performed on ions at m/z 240 for the identification of ions **B**. Two fragmental ions at m/z 212.1067 and 222.0911 helped us to confirm that **B** was the **2a** hydroperoxide (1-hydroperoxy-2-phenyl-3,4-dihydroisoquinolin-2-ium, **6a**) (Figure S8). In addition, accurate m/z of ions **C** was calculated to be $C_{15}H_{16}NO_4^+$ (error -2.2 ppm), which was protonated **1a** dihydroperoxide (1,1-dihydroperoxy-2-phenyl-1,2,3,4-tetrahydroisoquinoline, **7a**) deduced to be the precursor of oxidation product 2-phenyl-3,4-dihydroisoquinolin-1(2H)-one **4a**. According to the above

View Article Online
DOI: 10.1039/C9CC09630A

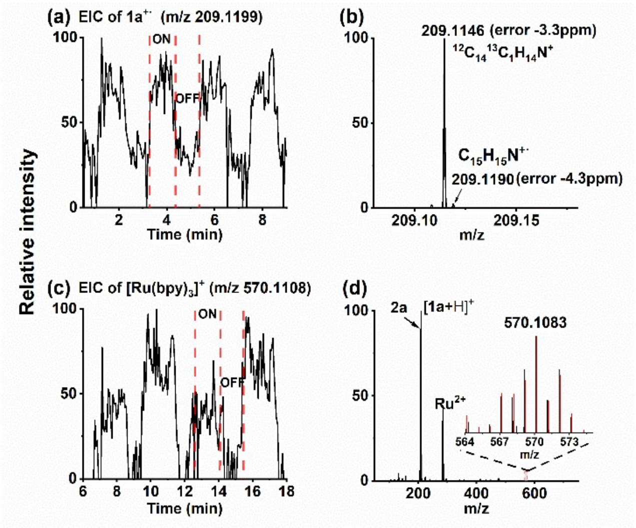

Figure 3. (a) EIC of $1a^{+\bullet}$; (b) Mass spectrum of $1a^{+\bullet}$ (m/z 209.1190) compared with the 2a-C^{13} (m/z 209.1146); (c) EIC of $Ru^{+}(bpy)_3$; (d) Mass spectrum of $Ru^{+}(bpy)_3$ with the insetting red line of theoretical isotopic peek.

results, it was clearly confirmed that the oxidation pathway forming amide involved a two-step dehydrogenation process. Density functional theory (DFT) calculation was carried out to investigate the possibility of the intermediates and the two-step dehydrogenation pathway (S5 section of SI). The relative Gibbs free energy (*G*) of the two-step dehydrogenation pathway at 298 K and 1 atm pressure in Eq S2–S6 was demonstrated in Figure 2. The calculation results presented that change of the Gibbs free energy (Δ*G*) from **5a** to **6a** was the only positive one while that of every other step was negative, which suggested that the dehydrogenation probably was started with PCET mechanism through reacting with $^1O_2$ produced from the $^3O_2$ under the visible light catalysis (Eq S3). This hinted that nearly all the processes (except for Eq S3) were energy favourable and the proposed two-step dehydrogenation mechanism was reasonable in terms of thermodynamics. These simulation results supported the possibility of the formation of **6a** and **7a** intermediates in the two-step dehydrogenation pathway.

What is more, another product ion at m/z 224.1065 was also found in the mass spectrum, corresponding to the oxidation product, protonated **4a** (CID MS/MS spectrum, Figure S9). For further confirmation of the correlation between the product ions and the laser irradiation, EIC was performed and presented in Figure 1c. All above detected ions came up along with the periodic laser irradiation in real time. And the calculated and measured m/z for THIQ and related substances were listed in Table 1. For the confirmation of the universality of this mechanism, reaction system was extended by using the *N*-methylaniline and *N*-ethylaniline and similar results were achieved (S3&S4 in SI).

In previous study, limited by the detection approaches, THIQ radical cation $\mathbf{1a}^{+\bullet}$ and reduced Ru catalyst $Ru^{+}(bpy)_3$ has not been specifically detected. The low concentration of reactants and the oxidation from the air maybe the main reason for no results by aforementioned experiments. Through combination of anaerobic experiment with our MS platform (S1 in SI), those intermediates were not only successfully detected but also confirmed. In detail, after 1 mM THIQ and 5 µM $[Ru(II)(bpy)_3]Cl_2$ were introduced to the system, the ions $\mathbf{1a}^{+\bullet}$ was detected, whose intensity changed along with the laser on/off status (Figure 3a, b). Furthermore, $Ru^{+}(bpy)_3$ was detected under periodical irradiation by magnifying ten-fold of the concentration of $[Ru(II)(bpy)_3]Cl_2$, from 5 µM to 50 µM (Figure 3c), which matched well with its theoretical isotopic peak distribution(marked in red line, inset of Figure 3d).

Based on all the above intermediates we discovered in this study, a modified and detailed mechanism was proposed (Scheme 2). For the visible-light photocatalyzed oxidation and C-H functionalization of THIQ, the reaction is initiated by the reductive quenching of photoexcited state of $Ru(bpy)_3Cl_2$ upon light irradiation by the THIQ **1a** to generate the THIQ amine radical $\mathbf{1a}^{+\bullet}$ and reduced $Ru^{+}(bpy)_3$. Then, $Ru^{+}(bpy)_3$ is oxidized by oxygen to complete photocatalytic cycle, producing the superoxide anion free radical, which abstract one hydrogen from $\mathbf{1a}^{+\bullet}$ to form THIQ iminium cation **2a** with counter ion OOH^-. Subsequently, the reaction has two paths to produce different products. With nucleophilic group OCH_3^-, C-H functionalization product **3a** will be generated from **2a** by nucleophilic addition. Importantly, **5a** (produced from **2a** with counter ion OOH^-) will participate in another visible light mediated PCET process to produce the intermediate **6a**, which contributes to the formation of **7a** and sequential final amide product **4a**. This unique two-step dehydrogenation process for the oxidation of THIQ under the condition of visible-light photoredox catalysis could be deduced from the captured intermediates for the first time.

Adopting THIQ as model substrate, the photocatalytic oxidation and functionalization process of C-H bonds adjacent to nitrogen was illuminated unambiguously and integrally by tracing the detailed reaction intermediates using online ESI-MS assisted with laser irradiation. Most importantly, two new peroxide addition intermediates involved in the process of amide product formation were captured for the first time, which discovered the two-step dehydrogenation process

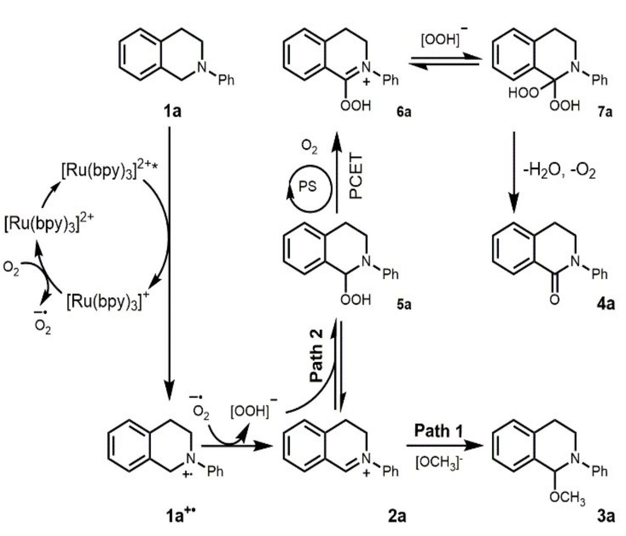

Scheme 2. Proposed mechanism of the oxidation and C-H functionalization of THIQ.

View Article Online
DOI: 10.1039/C9CC05629A

involved in PCET for the oxidation of THIQ. Furthermore, the comprehensive mechanism of co-existing pathways was confirmed by the detection of the transient iminium cation (peroxide adduct), amide product, methoxylated adduct, amine radical cations, the reduced photocatalyst Ru^{+}(bpy)$_3$ in real time. It is undeniable that ambient MS technique is an effective tool to make up the shortages of NMR. We hope more distinguished work can be realized using this device.

We sincerely thank Mr. Chenlong Li and Ms. Yiming Liu for their support and useful discussion in the theoretical calibration. This work was financially supported by the Chinese Ministry of Science and Technology (2016YFF0100303), and National Natural Science Foundation of China (Grant Nos 21874003, 21527809).

Conflicts of interest

There are no conflicts of interest to declare.

References

1. S. A. Girard, T. Knauber and C.-J. Li, *Angew. Chem. Int. Ed.*, 2014, **53**, 74-100.
2. M.-L. Louillat and F. W. Patureau, *Chem. Soc. Rev.*, 2014, **43**, 901-910.
3. A. E. Wendlandt, A. M. Suess and S. S. Stahl, *Angew. Chem. Int. Ed.*, 2011, **50**, 11062-11087.
4. V. R. Pattabiraman and J. W. Bode, *Nature*, 2011, **480**, 471.
5. L. Marzo, S. K. Pagire, O. Reiser and B. König, *Angew. Chem. Int. Ed.*, 2018, **57**, 10034-10072.
6. C. K. Prier, D. A. Rankic and D. W. C. MacMillan, *Chem. Rev.*, 2013, **113**, 5322-5363.
7. T. P. Yoon, *ACS Catal*, 2013, **3**, 895-902.
8. J.-R. Chen, X.-Q. Hu, L.-Q. Lu and W.-J. Xiao, *Acc. Chem. Res.*, 2016, **49**, 1911-1923.
9. N. A. Romero and D. A. Nicewicz, *Chem. Rev.*, 2016, **116**, 10075-10166.
10. B. König, *Eur. J. Org. Chem.*, 2017, 1979-1981.
11. A. G. Condie, J. C. Gonzalez-Gomez and C. R. Stephenson, *J. Am. Chem. Soc.*, 2010, **132**, 1464-1465.
12. M. Rueping, C. Vila, R. M. Koenigs, K. Poscharny and D. C. Fabry, *Chem. Commun.*, 2011, **47**, 2360-2362.
13. G. Zhao, C. Yang, L. Guo, H. Sun, C. Chen and W. Xia, *Chem. Commun.*, 2012, **48**, 2337-2339.
14. H. Wang, Y. Man, K. Wang, X. Wan, L. Tong, N. Li and B. Tang, *Chem. Commun.*, 2018, **54**, 10989-10992.
15. A. A. Guryev, F. Hahn, M. Marschall and S. B. Tsogoeva, *Chem. Eur. J.*, 2019, **25**, 4062-4066.
16. X. Z. Wang, Q. Y. Meng, J. J. Zhong, X. W. Gao, T. Lei, L. M. Zhao, Z. J. Li, B. Chen, C. H. Tung and L. Z. Wu, *Chem. Commun.*, 2015, **51**, 11256-11259.
17. J.-J. Zhong, C.-J. Wu, Q.-Y. Meng, X.-W. Gao, T. Lei, C.-H. Tung and L.-Z. Wu, *Adv. Synth. Catal.*, 2014, **356**, 2846-2852.
18. J. J. Zhong, Q. Y. Meng, B. Liu, X. B. Li, X. W. Gao, T. Lei, C. J. Wu, Z. J. Li, C. H. Tung and L. Z. Wu, *Org. Lett.*, 2014, **16**, 1988-1991.
19. T. Wang, M. Schrempp, A. Berndhauser, O. Schiemann and D. Menche, *Org. Lett.*, 2015, **17**, 3982-3985.
20. J. Xuan, T. T. Zeng, Z. J. Feng, Q. H. Deng, J. R. Chen, L. Q. Lu, W. J. Xiao and H. Alper, *Angew. Chem. Int. Ed.*, 2015, **54**, 1625-1628.
21. H. Bartling, A. Eisenhofer, B. König and R. M. Gschwind, *J. Am. Chem. Soc.*, 2016, **138**, 11860-11871.
22. A. A. Sabino, A. H. L. Machado, C. R. D. Correia and M. N. Eberlin, *Angew. Chem. Int. Ed.*, 2004, **43**, 2514-2518.
23. C. A. Marquez, F. Fabbretti and J. O. Metzger, *Angew. Chem. Int. Ed.*, 2007, **46**, 6915-6917.
24. C. Iacobucci, S. Reale and F. De Angelis, *Angew. Chem. Int. Ed.*, 2016, **55**, 2980-2993.
25. J. A. Willms, H. Gleich, M. Schrempp, D. Menche and M. Engeser, *Chem. Eur. J.*, 2018, **24**, 2663-2668.
26. Y. Wang, M. Sun, J. Qiao, J. Ouyang and N. Na, *Chem Sci*, 2018, **9**, 594-599.
27. J. Deng, Y. Yang, Y. Liu, L. Fang, L. Lin and T. Luan, *Anal Chem*, 2019, **91**, 4592-4599.
28. L. S. Santos, *European Journal of Organic Chemistry*, 2008, **2008**, 235-253.
29. T. A. Brown, H. Chen and R. N. Zare, *J Am Chem Soc*, 2015, **137**, 7274-7277.
30. T. A. Brown, H. Chen and R. N. Zare, *Angew. Chem. Int. Ed.*, 2015, **54**, 11183-11185.
31. Q. Zheng, Y. Liu, Q. Chen, M. Hu, R. Helmy, E. C. Sherer, C. J. Welch and H. Chen, *J. Am. Chem. Soc.*, 2015, **137**, 14035-14038.
32. T. A. Brown, N. Hosseini-Nassab, H. Chen and R. N. Zare, *Chem Sci*, 2016, **7**, 329-332.
33. X. Yan, R. M. Bain and R. G. Cooks, *Angew. Chem. Int. Ed.*, 2016, **55**, 12960-12972.
34. S. Banerjee, Y. F. Yang, I. D. Jenkins, Y. Liang, A. A. Toutov, W. B. Liu, D. P. Schuman, R. H. Grubbs, B. M. Stoltz, E. H. Krenske, K. N. Houk and R. N. Zare, *J. Am. Chem. Soc.*, 2017, **139**, 6880-6887.
35. Y. Cai, J. Wang, Y. Zhang, Z. Li, D. Hu, N. Zheng and H. Chen, *J. Am. Chem. Soc.*, 2017, **139**, 12259-12266.
36. N. Zeng, Z. Long, Y. Wang, J. Sun, J. Ouyang and N. Na, *Anal Chem*, 2019, **91**, 15763-15768.
37. R. Horn, K. A. Williams, N. J. Degenstein and L. D. Schmidt, *Chemical Engineering Science*, 2007, **62**, 1298-1307.
38. A. Goguet, C. Hardacre, N. Maguire, K. Morgan, S. O. Shekhtman and S. P. Thompson, *Analyst*, 2011, **136**, 155-163.
39. K. Morgan, N. Maguire, R. Fushimi, J. T. Gleaves, A. Goguet, M. P. Harold, E. V. Kondratenko, U. Menon, Y. Schuurman and G. S. Yablonsky, *Catalysis Science & Technology*, 2017, **7**, 2416-2439.
40. S. Chen, Q. Wan and A. K. Badu-Tawiah, *Angew. Chem. Int. Ed.*, 2016, **55**, 9345-9349.